Effects of Conformational Distributions on Sigma Profiles in COSMO Theories

Shu Wang,[†] John M. Stubbs,[‡] J. Ilja Siepmann,[§] and Stanley I. Sandler*,[†]

Center for Molecular and Engineering Thermodynamics, Department of Chemical Engineering, University of Delaware, Newark, Delaware 19716, Department of Chemistry, Grinnell College, Grinnell, Iowa 50112, and Departments of Chemistry and of Chemical Engineering and Materials Science, University of Minnesota, Minneapolis, Minnesota 55455

Received: July 13, 2005; In Final Form: September 28, 2005

The charge density or sigma profile of a solute molecule is an essential component in COSMO (conductor-like screen model) based solvation theories, and its generation depends on the molecular conformation used. The usual procedure is to determine the conformation of an isolated molecule, and assume that this is unchanged when the molecule is placed in solution. In this paper, the conformations of 1-hexanol and 2-methoxy-ethanol in both the liquid and vapor phases obtained from Gibbs ensemble simulation and from an isolated-molecule quantum DFT optimization are used to determine the effect of realistic conformation differences on COSMO-based properties predictions. In particular, the vapor pressure at the normal boiling temperature and the binary mixture VLE (vapor-liquid equilibrium) predictions obtained using different conformations are investigated. The results show that the sigma profile for 1-hexanol varies only slightly using the different conformations, while the sigma profile of 2-methoxy-ethanol shows a significant difference between the liquid and vapor phases. Consequently, the vapor pressure predictions for 1-hexanol are similar regardless of the manner in which the conformation population was obtained, while there is a larger difference for 2-methoxy-ethanol depending on whether the liquid or vapor conformations from simulation or the DFT-optimized structure is used. These differences in predictions are seen to be largely due to differences in the ideal solvation energy term. In mixture VLE calculations involving 1-hexanol, we again see that there is little difference in the phase equilibrium predictions among the different conformations, while for the mixture with 2-methoxy-ethanol, the differences in the sigma profiles lead to a more noticeable, though not significant, difference in the phase equilibrium predictions.

1. Introduction

The thermodynamic properties of chemicals in condensed phases are much different from those in the gas phase as a result of close packing, solvation, and strong interactions. Different approaches have been used to estimate the thermodynamic properties in condensed phases. Empirical group contribution methods (GCM)[1] allow the prediction of properties of pure compounds and mixtures based on models with parameters derived from reliable experimental data. Descriptors other than structural groups have been used in quantitative structure−property relationship (QSPR) models.[2] Also, computer simulation,[3] such as in Monte Carlo (MC) and molecular dynamics (MD) techniques, has been used to calculate thermodynamic properties of liquids in which the solvent is treated explicitly, frequently using interactions between molecules described by semiempirical force fields. Such a treatment requires extensive computational time because of the large number of degrees of freedom. Instead of explicit solvent models, continuum solvation models (CSM),[4,5] like COSMO (conductor-like screening model), developed by Klamt,[6,7] treat the solvent implicitly as a homogeneous continuous polarizable medium characterized by a single physical property, the dielectric constant.

In COSMO theory, the solute is placed in a cavity of a continuum medium with dielectric ϵ equal to infinity to model a perfect conductor. The shape of the cavity is defined by the contour of the solvent accessible surface based on the conformation of the molecule and the van der Waals radii of the atoms. Then segments with screening charges on the cavity boundary resulting from polarization by the solvent are calculated iteratively using a self-consistent reaction field (SCRF) model. Since the surface shape is more complex than spherical or ellipsoidal in the COSMO theory, a numerical rather than analytical representation is required, and different cavity shapes result in different screening charges distributed over the surface of the molecule. Using the charge density on surface elements of fixed size, a sigma profile is constructed to quantitatively represent the charge distribution on the molecular surface. The sigma profile gives the probability $p(\sigma)$ of finding a surface area segment with a charge density, σ, where $p(\sigma)$ is defined as ratio of the number of segments with charge density σ to the total number of surface segments of the molecule. From the sigma profile, the free energy required to change the environment from a perfect conductor to real solvent can be calculated, and this is referred to as the restoring free energy.

Combining the restoring free energy with the free energy required to create a cavity, and the dispersion free energy that is proportional to the exposed surface area of the different atom types, COSMO theory can be used to predict vapor pressures and enthalpies of vaporization.[8] Or, with the free energy difference between a molecule in a liquid mixture and in its pure liquid, vapor−liquid equilibrium can be predicted.[9] COSMO theory has also been used in the prediction of soil sorption

[†] University of Delaware.
[‡] Grinnell College.
[§] University of Minnesota.

10.1021/jp053859h CCC: $30.25
Published on Web 11/19/2005

coefficients,[10] pK_a values,[11] and infinite dilution activity coefficients[12] and in many other applications.

The construction of the sigma profile is the key step in COSMO theory and requires the most computational time. It is critical to obtain an accurate sigma profile in order to properly describe the charge density distribution. The shape of the cavity of a molecule will affect the charge density distribution, and therefore affect the sigma profile, so that determining the correct conformation of a molecule is important in the COSMO theory, especially for flexible molecules. However, even small molecules can have numerous conformations resulting in different shapes and solvation free energies. A straightforward way to select the structure of a solute molecule is by choosing the geometry with lowest energy, though this can be difficult if there are many conformations with different structures but similar energies. Klamt[13] suggested that averaging over several conformers using a Boltzmann-weighting algorithm and iterating over the occupation numbers of different conformations for each temperature until consistency is reached should be used, but there are no further details available about this weighting strategy. Another important issue is the essential approximation[6] in COSMO theory that the structure of the solute is unchanged going from the gas phase to the perfect conductor phase, and then to the real solvent.

Here we have tested this last assumption by calculating sigma profiles for ensembles of molecules in the vapor phase and, separately, in the liquid phase obtained from simulation. These sigma profiles are then compared to see if changes in the phase (and therefore the local environment) result in differences in molecular conformations, and how this affects thermodynamic property predictions. We have also compared average sigma profiles for vapor and liquid structures obtained from Monte Carlo simulation with the sigma profile found in the usual manner in COSMO-based methods, which is from the structure obtained using quantum DFT optimization.

2. Computational Details

Structures from Different Cases. In this study two chemicals, 1-hexanol and 2-methoxy-ethanol, are investigated. 1-Hexanol was picked as an example of a relatively simple polar molecule, while 2-methoxy-ethanol was chosen because it can form intramolecular hydrogen bonds and is more polar than 1-hexanol. To obtain ensembles of molecules representing typical vapor and liquid phase conformations, configurational-bias Monte Carlo simulations[14,15] in the Gibbs ensemble[16] were carried out at temperatures of 443 and 450 K for 1-hexanol and 2-methoxy-ethanol. The united-atom version of the TraPPE (transferable potentials for phase equilibria) force field[17−19] was used for both simulations. For 1-hexanol, a total of 200 molecules and a total volume of 997941 Å^3 were used, resulting in about 163 molecules with a molar volume of 1.48×10^{-4} m^3/mol in the liquid phase and about 37 molecules with a molar volume of 1.60×10^{-2} m^3/mol in the vapor phase. For 2-methoxy-ethanol, the total number of molecules and volume were 250 and 519160 Å^3, respectively. The corresponding average numbers of molecules and molar volumes for the liquid and vapor phase are 202 molecules with 9.69×10^{-5} m^3/mol and 48 molecules with 6.08×10^{-3} m^3/mol, respectively. For each chemical, 10 instantaneous configurations (or snapshots) of all the molecules in the liquid and vapor phases (spaced at 5000 MC cycles) were collected and the positions of the nonpolar hydrogen atoms were added using simple geometric considerations for the subsequent calculation of the sigma profiles. The sigma profiles for all the molecules in a single snapshot of a given phase are computed. The average sigma profiles from these ensembles (either using a single snapshot or the average of all 10 snapshots) were used in the COSMO calculations, and the predictions of the thermodynamic properties based on these ensembles are compared with the calculation using the sigma profile from a single molecule DFT-optimized structure.

COSMO Calculation. The COSMO method implemented in Jaguar 5 with density functional theory (DFT) was used for the quantum mechanics (QM) calculation. The geometry of each of the molecules in an ensemble is used in the COSMO solvation calculation (isolv = 3), which is performed at the B3LYP/6-31+G** level. The solvation cavity is determined using the Connolly algorithm, and is represented by a set of points with a density of 4 points/Å^2 (cosfden = 4). The values of the solute atomic radii (vdw2) are the same as in ref 8, and a probe of radius 1.57 Å (radprb = 1.57, same as the hydrogen radius) is used. Ultrafine grid and tight cutoffs are used (iacc = 1). The escaping charges are corrected using the double shell method of Klamt and Jonas[20] with the outer shell thickness set to 90% of rprobe (cskin = 1.413). The time of the COSMO calculation is about 10 min for a single 1-hexanol or 2-methoxy-ethanol molecule on a Linux machine with an AMD 1800+ CPU.

Thermodynamic Properties Predictions. The equations for the vapor pressure prediction at the normal boiling temperature are as described earlier:[8]

$$\ln P_i^{\mathrm{vap}} = \frac{\Delta G_{i/i}^{*\mathrm{sol}}}{RT} + \ln \frac{RT}{V_{i/\mathrm{L}}} - \ln \frac{f(T,P_i^{\mathrm{vap}})}{P_i^{\mathrm{vap}}} \qquad (1)$$

where $\Delta G_{i/i}^{*\mathrm{sol}}$ is the solvation Gibbs energy, $V_{i/\mathrm{L}}$ is the liquid molar volume of species i, and f is the fugacity that here is equal to the vapor pressure since we assume that vapor phase is ideal as all the calculations are done near atmospheric pressure.

The solvation Gibbs energy is a result of the electrostatic and polarization interactions between the molecules, which consists of van der Waals dispersion free energy and electrostatic free energy:

$$\Delta G_{i/i}^{*\mathrm{sol}} = \Delta G_{i/i}^{*\mathrm{vdw}} + \Delta G_{i/i}^{*\mathrm{el}} \qquad (2)$$

The van der Waals free energy has cavity formation and dispersion contributions that can be expressed in terms of the Helmholtz energy as follows:

$$\frac{\Delta G_{i/i}^{*\mathrm{vdw}}}{RT} = \frac{\Delta A_{i/i}^{*\mathrm{disp}}}{RT} + \frac{\Delta A_{i/i}^{*\mathrm{cav}}}{RT} - 1 \qquad (3)$$

The Helmholtz energy of cavity formation is modeled using an expression from thermodynamic perturbation theory:[21,22]

$$\frac{\Delta A_{i/i}^{*\mathrm{cav}}}{RT} = (2\alpha - 1)\frac{\eta(4-3\eta)}{(1-\eta)^2} - (2\alpha - 2)\ln\left[\frac{1-\eta/2}{(1-\eta)^3}\right] \qquad (4)$$

where α is an sphericity parameter and η is the packing fraction.

The dispersion term was obtained using a first-order mean field approximation to account for all possible pairwise interactions between the atoms in different molecules:

$$\frac{\Delta A_{i/i}^{*\mathrm{disp}}}{RT} = \frac{\sum_j \sum_k \epsilon_{jk} m_j^i m_k^i}{RT_{i/\mathrm{L}}} \qquad (5)$$

where $\epsilon_{jk} = (\epsilon_j\epsilon_k)^{1/2}$ is pair-interaction energy between atom type j and atom type k, and has units of energy times volume, and m_j^i is the effective number of atoms of type j within a species i molecule obtained from

$$m_j^i = \sum_{a\in j}\left(\frac{S_a}{S_{a0}}\right)^q \tag{6}$$

where S_a is the exposed surface area, or solvent accessible area, of atom a and S_{a0} is the bare surface area calculated using the set of atomic radii (R_{el}), which are used in the QM calculations.

As in ref 8 the electrostatic free energy is obtained as follows:

$$\Delta G_{i/i}^{*el} = \Delta G_{i/i}^{*is} + \Delta G_{i/i}^{*cc} + \Delta G_{i/i}^{*res} \tag{7}$$

where $\Delta G_{i/i}^{*is}$ is the absolute energy difference of the molecule between ideal conductor and the ideal gas phase, and $\Delta G_{i/i}^{*cc}$ is the correction to the free energy due to the charge averaging processes in which each segment calculated from quantum mechanics is reorganized into standard segments. Also, $\Delta G_{i/i}^{*res}$ is the restoring Gibbs energy required to change from the ideal conductor state to the real liquid state, and is calculated from the sigma profile or charge density as described in ref 8.

For vapor−liquid-equilibrium predictions, the activity coefficients for species i in solvent S can be expressed as before:[9]

$$\ln \gamma_{i/S} = \frac{\Delta G_{i/S}^{*res} - \Delta G_{i/i}^{*res}}{RT} + \ln \gamma_{i/S}^{SG} \tag{8}$$

where

$$\ln \gamma_i^{SG} = \ln\frac{\phi_i}{x_i} + \frac{z}{2}q_i \ln\frac{\theta_i}{\phi_i} + l_i - \frac{\phi_i}{x_i}\sum_j x_j l_j \tag{9}$$

is the combinational term calculated using the Staverman−Guggenheim model that accounts for molecular size and shape differences.

The residual term becomes important when polar molecules are involved, and is obtained as the difference between the restoring free energy in a mixture and in a pure fluid, which can be calculated from COSMO−SAC theory. The restoring free energy is

$$\frac{\Delta G_{i/i}^{*\,res}}{RT} = n\sum_{\sigma_m} p(\sigma_m) \ln \Gamma_i(\sigma_m) \tag{10}$$

and

$$\ln \Gamma_S(\sigma_m) = -\ln\left\{\sum_{\sigma_n} p_S(\sigma_n)\Gamma_S(\sigma_n) \exp\left[\frac{-\Delta W(\sigma_m,\sigma_n)}{RT}\right]\right\} \tag{11}$$

For mixtures, the sigma profiles are obtained as the sum of the sigma profiles of each compound weighted by their mole fractions (x_i) and surface areas (A_i):

$$p_S(\sigma) = \frac{\sum_i x_i n_i p_i(\sigma)}{\sum_i x_i n_i} = \frac{\sum_i x_i A_i p_i(\sigma)}{\sum_i x_i A_i} \tag{12}$$

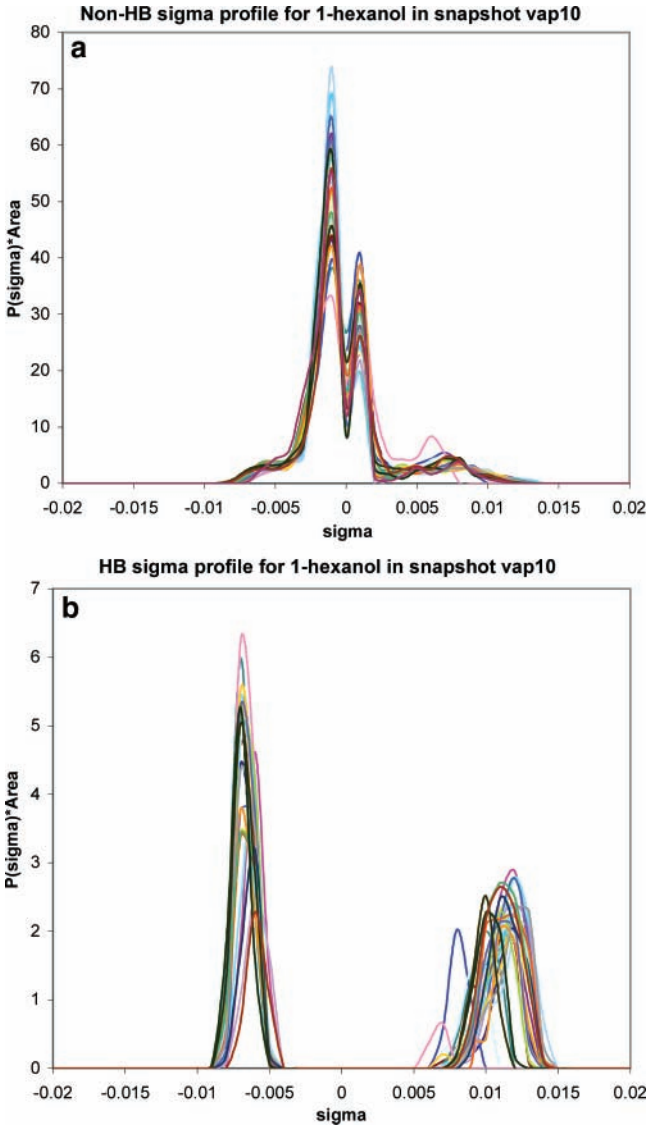

Figure 1. Sigma profiles for the non-hydrogen-bonding (top) and hydrogen-bonding (bottom) parts of 1-hexanol. The individual profiles for all 29 1-hexanol molecules in snapshot 10 of the vapor phase are shown in different colors.

The numbers of parameters and their values in this model are the same as in ref 8, in which 13 dispersion coefficients for specified atom and bonding types are used.

3. Results and Discussions

Effect of Conformation on the Sigma Profiles. Since the sigma profiles depend on the positions of the atomic nuclei and the molecular orbitals of a single molecule, the sigma profile will be different in different conformations of the molecule. As an example, Figures 1a and 1b show the sigma profiles for the non-hydrogen-bonding (nonpolar) and hydrogen-bonding parts of the 1-hexanol molecules in the vapor phase for the different conformations found in snapshot 10. The sigma profiles for the non-hydrogen-bond atoms, which, in this case, consists of six carbon atoms and thirteen hydrogen atoms, have two peaks near zero, one in the negative region, and the other in the positive region, resulting from the exposed hydrogen and carbon surfaces, respectively. The different positions of the nuclei in the various conformations found in simulation lead to variations in the exposed surface areas for these hydrogen and carbon atoms from one molecule to the next in the ensemble, and

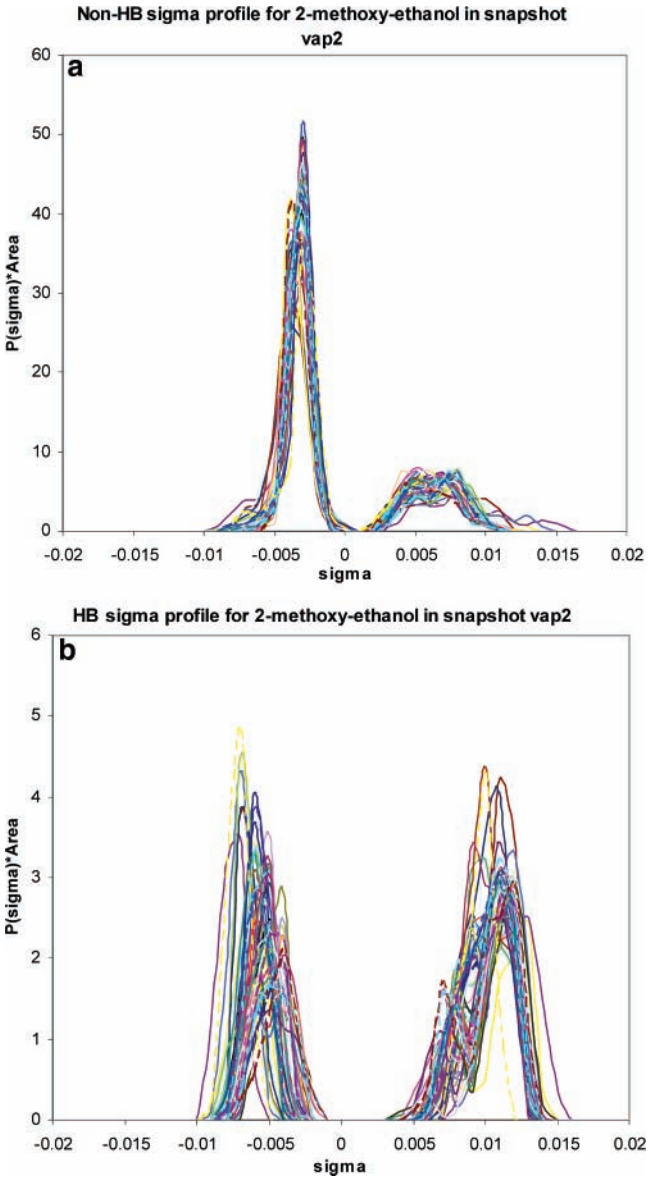

Figure 2. Sigma profiles for the non-hydrogen-bonding (top) and hydrogen-bonding (bottom) parts of 2-methoxy-ethanol. The individual profiles for all 64 molecules in snapshot 2 of the vapor phase are shown in different colors and line styles.

therefore to different peak values. Note that the small plateaus after the peak in the positive part of the sigma profile, and before the peak in the negative part, quantitatively show how much the hydroxyl group affects the neutral hexyl group as a result of polarization.

The sigma profile for the hydrogen bond part of the molecule is a result of the contributions from the oxygen (and more generally in other molecules also from the nitrogen and fluorine) atoms, and from the hydrogen atoms directly connected to these atoms, as defined in ref 8. As a result of the different H-bond angles, two pronounced peaks corresponding to hydrogen (negative peak) and oxygen (positive peak) have different values and positions in the sigma profiles corresponding to different conformations. However, they all show broad peaks as a result of the hydroxyl group that has a large surface charge density.

Figure 2a shows the non-hydrogen-bonding sigma profiles for 2-methoxy-ethanol in the vapor phase of snapshot 2. There we see that 2-methoxy-ethanol has one small positive, but broad area instead of the sharp peak found with 1-hexanol, since here the exposed surface area of the three carbon atoms is mostly covered by the adjoining hydrogen atoms and the ether oxygen. Not only has the surface area changed, but the contribution from the carbon atoms has also shifted from a sigma value near zero to a more positive value, quantitatively reflecting the fact that the electron acceptors in 2-methoxy-ethanol, with both ether and hydroxyl oxygen atoms, result in a greater attractive shift of the electron densities from the neutral atoms than is the case for the single acceptor in 1-hexanol.

Figure 2b shows the hydrogen-bonding part of the sigma profile. The two almost equal peaks at positive and negative sigma values indicate that the two oxygen atoms have similar exposed surface areas to that of the hydroxyl hydrogen atom. Figures 3 and 4 for 1-hexanol and 2-methoxy-ethanol, respectively, show the average sigma profiles calculated using the conformations in the liquid and vapor phases obtained from simulation, and from the optimized structure found from the DFT calculations.

Figures 3a and 3b show the averaged non-HB (non-hydrogen-bonding) and HB sigma profiles obtained for conformations from the ensemble of liquid conformations for 1-hexanol obtained using a linear weighting of the conformers within one snapshot. [Since the configurations are taken directly from the Monte Carlo simulations, each snapshot has the same statistical weight and conformers should appear with their correct probabilities. Thus, one should not use a post-simulation Boltzmann weighting for these conformers.] It is interesting to note that the averaged sigma profiles from each of the different liquid ensembles are almost identical. The results show that linearly averaging the sigma profiles of many equilibrium conformations in the liquid and vapor states separately (and even from different ensembles), we obtain similar "averaged structures" and nearly identical average surface charge density distributions. The same can be seen in Figures 3c and 3d for the vapor phase ensembles in that there is only a small change in the peak (oxygen atom surface charge density) in the positive sigma range of the hydrogen-bonding sigma profile from conformations of the different ensembles. Similarly, the average sigma profiles for 3-methoxy-ethanol show little difference between different snapshots for a given phase (see Figures 4a to 4d).

Next we compare the sigma profiles calculated from structures in liquid ensembles, vapor ensembles, and the density-functional optimized structures. As Figures 3e and 3f show, for 1-hexanol, the averaged sigma profiles calculated from the liquid ensembles are almost the same as from the vapor ensembles, which indicates that the 1-hexanol "averaged structures" change little when the local environment changes from the vapor to the liquid phase. As a simple polar molecule with only one hydroxyl group, the structure of 1-hexanol mainly depends on the angles and orientations of carbon atom chain, which change little when the environment changes. However, 2-methoxy-ethanol is a more complex polar molecule and the "averaged structures" do change as the environment changes, although these changes have only a limited effect on the thermodynamic properties predictions as will be discussed in the next section.

When we compare the structures from the simulation ensembles and the DFT optimized structure, we see there are noticeable differences for both 1-hexanol and 2-methoxy-ethanol. The structure obtained from quantum mechanical geometry optimization is for an isolated molecule, that is, there is no solvation effect. With the six carbon atoms and the oxygen atom assuming an all-trans zigzag conformation, the optimal structure for 1-hexanol has a minimum exposed surface area of the carbon atoms and a maximum exposed area for the hydrogen atoms, which explains why in Figure 3e the sigma profile peak

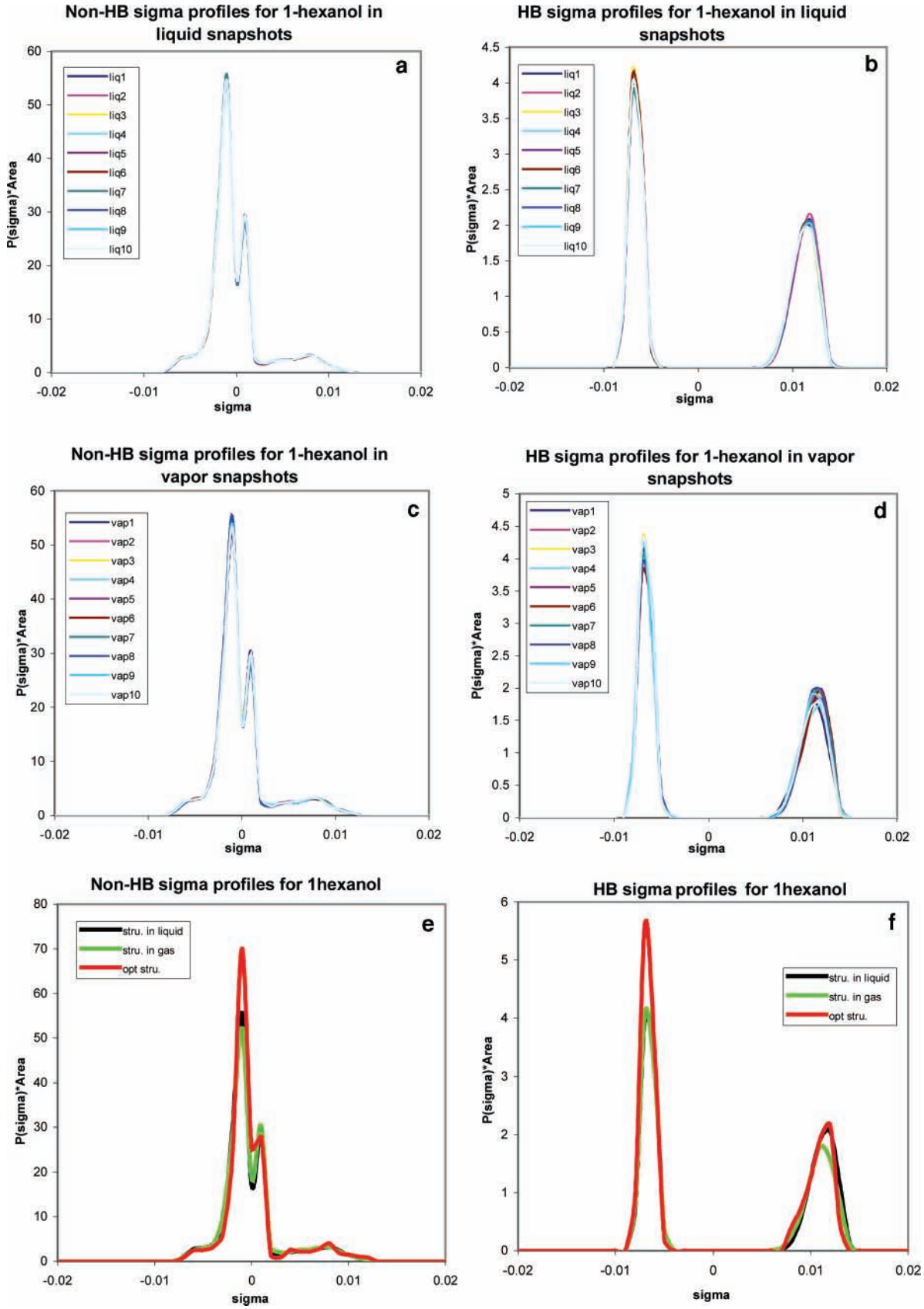

Figure 3. Sigma profiles for the non-hydrogen-bonding (left panel) and hydrogen-bonding (right panel) for 1-hexanol. The top and middle rows show the average profiles obtained for separate liquid- and vapor-phase snapshots, respectively. The bottom row depicts a comparison of the overall averages computed for the liquid and vapor phases and for the DFT conformation.

of carbon is lower and the peak of hydrogen is higher for the optimum structure than for those obtained from the simulations which contain a significant fraction of gauche defects, as should be expected at a temperature of about 450 K. Also, the structures obtained from simulation are based on the use of a molecular mechanics force field and not from quantum mechanical

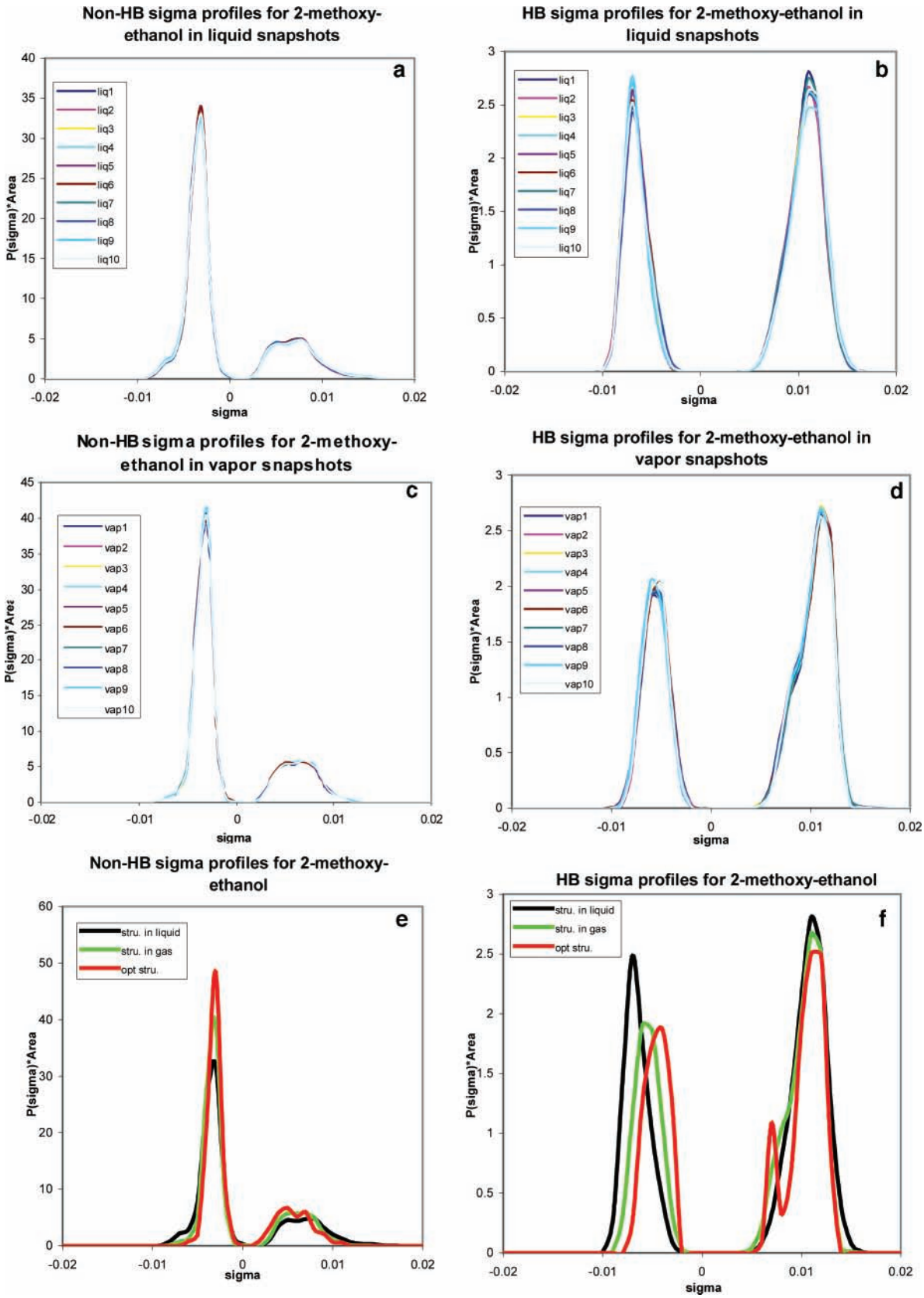

Figure 4. Sigma profiles for the non-hydrogen-bonding (left panel) and hydrogen-bonding (right panel) for 2-methoxy-ethanol. Plots are arranged as in Figure 3.

optimization, so that we would not expect the structures to be identical.

The three carbon and two oxygen atoms are also found in an all-trans zigzag conformation for the optimal 2-methoxy-ethanol structure with the lowest energies in both the liquid and vapor phases, which again leads to a maximum exposed hydrogen surface area. Comparing the sigma profiles, we see that for 2-methoxy-ethanol the profile from the optimum structure is more similar to the "averaged structures" from the vapor ensembles than from the liquid, as might be expected since the

TABLE 1: Vapor Pressure Prediction for 1-Hexanol

snapshot	no. of molecules	mean ln P_{vap}	mean $\Delta G_{i/i}^{*cco}/RT$	mean $\Delta G_{i/i}^{*dsp}/RT$	mean $\Delta G_{i/i}^{*res}/RT$	mean $\Delta G_{i/i}^{*cav}/RT$	ln(RT/V)
liq1	164	11.3969	−4.3194	−8.7890	2.9480	4.5331	17.0242
liq2	162	11.3817	−4.3062	−8.7685	2.9298	4.5148	17.0242
liq3	166	11.4294	−4.2522	−8.7945	2.9258	4.5260	17.0242
liq4	167	11.4062	−4.2808	−8.7964	2.9290	4.5302	17.0242
liq5	160	11.4395	−4.2573	−8.7775	2.9338	4.5288	17.0242
liq6	159	11.3836	−4.3201	−8.7885	2.9367	4.5314	17.0242
liq7	152	11.4268	−4.3026	−8.7854	2.9651	4.5256	17.0242
liq8	153	11.4078	−4.2834	−8.7749	2.9398	4.5021	17.0242
liq9	161	11.4154	−4.2723	−8.7822	2.9313	4.5144	17.0242
liq10	171	11.4239	−4.2685	−8.7767	2.9247	4.5318	17.0242
liquid av	1615	11.4111	−4.2863	−8.7834	2.9364	4.5238	17.0242
vap1	36	11.5227	−4.0903	−8.7990	2.9068	4.4810	17.0242
vap2	38	11.4475	−4.2419	−8.7780	2.9428	4.5004	17.0242
vap3	34	11.4166	−4.1843	−8.8043	2.8857	4.4953	17.0242
vap4	33	11.5711	−4.1274	−8.7928	2.8927	4.5745	17.0242
vap5	40	11.5015	−4.1934	−8.7838	2.9438	4.5107	17.0242
vap6	41	11.5214	−4.2510	−8.7715	2.9345	4.5851	17.0242
vap7	48	11.4326	−4.3106	−8.7919	2.9450	4.5659	17.0242
vap8	47	11.5080	−4.2597	−8.7916	2.9685	4.5667	17.0242
vap9	39	11.4527	−4.2752	−8.7944	2.9580	4.5401	17.0242
vap10	29	11.5062	−4.1625	−8.7772	2.9079	4.5138	17.0242
vapor av	385	11.4880	−4.2096	−8.7885	2.9286	4.5334	17.0242
DFT structure	1	11.5374	−4.3088	−8.8606	2.926	4.7566	17.0242

TABLE 2: Vapor Pressure Prediction for 2-Methoxy-ethanol

snapshot	no. of molecules	mean ln P_{vap}	mean $\Delta G_{i/i}^{*cco}/RT$	mean $\Delta G_{i/i}^{*dsp}/RT$	mean $\Delta G_{i/i}^{*res}/RT$	mean $\Delta G_{i/i}^{*cav}/RT$	ln(RT/V)
liq1	175	10.6905	−7.6331	−7.1471	4.2404	3.7915	17.4384
liq2	186	10.7583	−7.5217	−7.1519	4.1739	3.8197	17.4384
liq3	183	10.6825	−7.6407	−7.1448	4.2329	3.7968	17.4384
liq4	176	10.7385	−7.5900	−7.1565	4.2234	3.8233	17.4384
liq5	175	10.8055	−7.5318	−7.1516	4.2281	3.8225	17.4384
liq6	174	10.7233	−7.6047	−7.1498	4.2148	3.8247	17.4384
liq7	176	10.7529	−7.5665	−7.1498	4.2225	3.8084	17.4384
liq8	165	10.7370	−7.6430	−7.1473	4.2737	3.8152	17.4384
liq9	174	10.5376	−7.8945	−7.1439	4.3249	3.8127	17.4384
liq10	169	10.6567	−7.7212	−7.1462	4.2792	3.8065	17.4384
liquid av	1753	10.7083	−7.6347	−7.1489	4.2414	3.8121	17.4384
vap1	75	11.7394	−6.4639	−7.2005	3.8730	3.8517	17.4384
vap2	64	11.7439	−6.2134	−7.1626	3.9624	3.7191	17.4384
vap3	67	11.9168	−6.2479	−7.1665	3.9758	3.9171	17.4384
vap4	74	11.8554	−6.2263	−7.1641	3.9638	3.8437	17.4384
vap5	75	11.8942	−6.2496	−7.1581	3.9537	3.9098	17.4384
vap6	76	11.8121	−6.2890	−7.1641	3.9859	3.8410	17.4384
vap7	74	11.8449	−6.3483	−7.1574	4.0070	3.9054	17.4384
vap8	85	11.8405	−6.2699	−7.1603	3.9700	3.8624	17.4384
vap9	76	11.8269	−6.2651	−7.1715	3.9684	3.8569	17.4384
vap10	81	12.0225	−6.1798	−7.1544	3.9551	3.9632	17.4384
vapor av	747	11.8497	−6.2753	−7.1659	3.9615	3.8670	17.4384
DFT structure	1	12.4304	−5.4831	−7.1869	3.8028	3.8592	17.4384

optimum structure was computed for a vacuum, not for a solvated molecule in a condensed phase. Other than that, the sigma profiles from the optimum conformations show only modest differences from those obtained using the conformations found in simulation. Therefore, at least for the molecules we have considered, the single optimum structure sigma profile is a good approximation to that obtained from the averaged structure from simulation.

Structure Effect on Vapor Pressure Predictions. The sigma profile and the absolute energy for each molecule from the simulation ensembles were first calculated, and then the vapor pressure and its components (ideal solvation energy, dispersion energy, restoring energy, and cavity formation energy) for each molecule were evaluated. Finally, the sigma profiles and the logarithm of the vapor pressures for every ensemble were linearly averaged. Since here we predict vapor pressures at the normal boiling temperatures, the experimental value should be 101.325 kPa or 11.526 in natural log units. All the results are listed in Table 1 for 1-hexanol and Table 2 for 2-methoxy-ethanol. The COSMO methodology used here yields excellent results for the saturated vapor pressure of 1-hexanol irrespective of whether the prediction is based on the DFT conformation (P_{vap} is overestimated by 1%), the average liquid-phase conformation (P_{vap} is underestimated by 12%), or the average gas-phase conformation (P_{vap} is underestimated by 4%). The predictions for 2-methoxy-ethanol are in all three cases less satisfactory with the DFT and average gas-phase conformations yielding overestimations by a factor of 2.5 and 1.4, respectively, whereas P_{vap} is underestimated by a factor of 2.3 for the average liquid-phase conformation. It is interesting to note that for

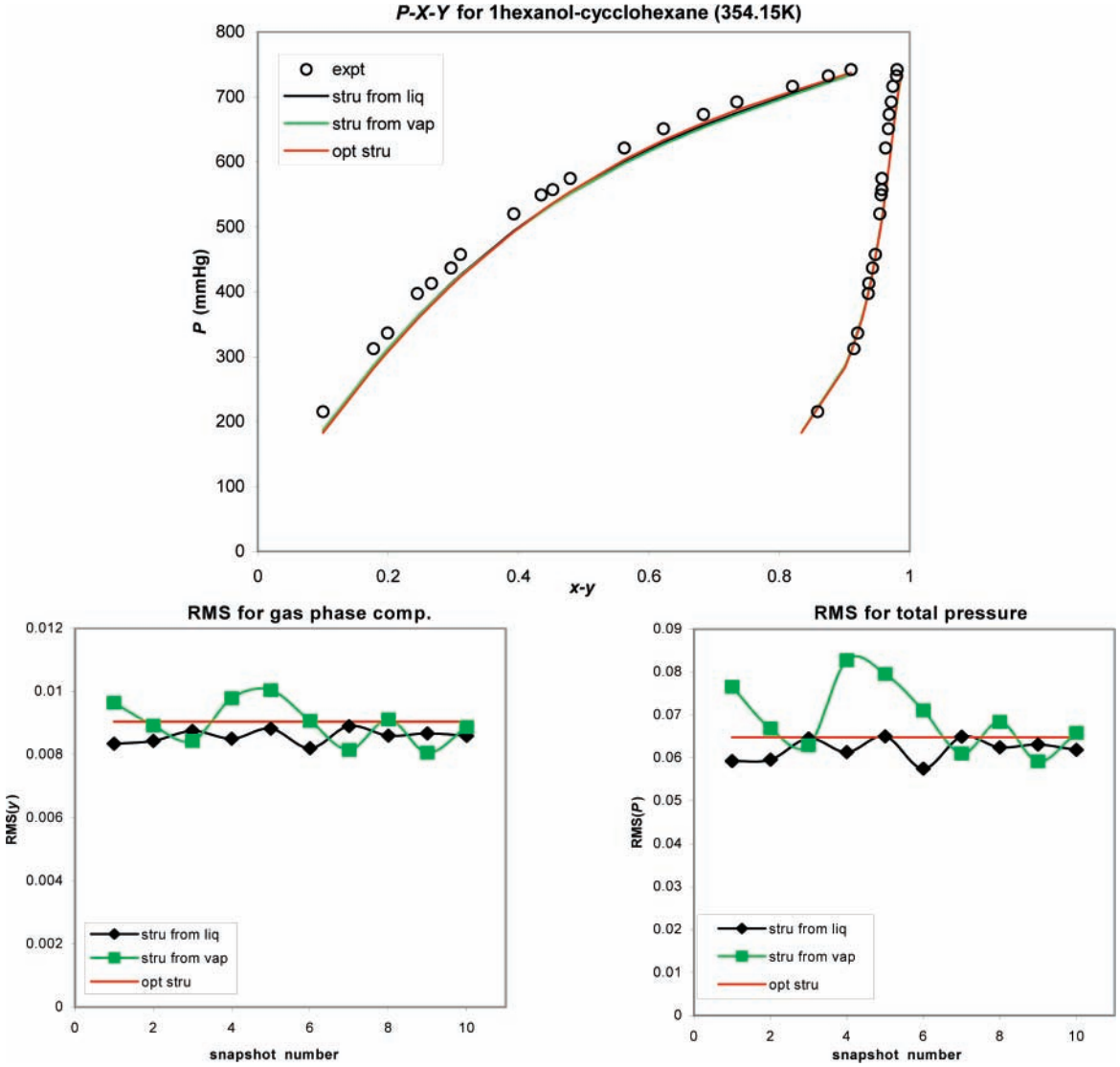

Figure 5. Pressure-composition projection and root-mean-square errors in the gas-phase composition (bottom left) and total pressure (bottom right) for the binary mixture of 1-hexanol and cyclohexane at $T = 354.15$ K. The experimental data are taken from ref 23.

TABLE 3: Free Energy Components for 2-Methoxy-ethanol

snapshot	no. of molecules	mean E_{COSMO} (kcal/mol)	mean E_{GAS} (kcal/mol)	mean $\Delta G_{i/i}^{*is}/RT$	mean $\Delta G_{i/i}^{*cc}/RT$
liq1	175	−169162.2694	−169155.0041	−9.1970	1.5639
liq2	186	−169162.7980	−169155.5894	−9.1272	1.6055
liq3	183	−169162.5617	−169155.2650	−9.2384	1.5976
liq4	176	−169163.1898	−169155.9333	−9.1870	1.5970
liq5	175	−169162.8243	−169155.6098	−9.1345	1.6027
liq6	174	−169163.0254	−169155.7591	−9.1985	1.5939
liq7	176	−169162.6836	−169155.4566	−9.1502	1.5837
liq8	165	−169163.1536	−169155.8901	−9.1962	1.5532
liq9	174	−169162.3500	−169154.8872	−9.4483	1.5538
liq10	169	−169162.6232	−169155.3049	−9.2655	1.5443
liquid av	1753	−169162.7479	−169155.4700	−9.2143	1.5796
vap1	75	−169165.3500	−169158.7200	−8.3919	1.9280
vap2	64	−169164.4803	−169158.2555	−7.8803	1.6669
vap3	67	−169164.0828	−169157.8519	−7.8884	1.6404
vap4	74	−169164.0586	−169157.8181	−7.9019	1.6756
vap5	75	−169163.7815	−169157.5060	−7.9445	1.6949
vap6	76	−169163.7762	−169157.5055	−7.9395	1.6505
vap7	74	−169163.7038	−169157.3528	−8.0399	1.6915
vap8	85	−169163.8305	−169157.5540	−7.9473	1.6774
vap9	76	−169164.3583	−169158.0580	−7.9759	1.7107
vap10	81	−169163.7475	−169157.5263	−7.8763	1.7005
vapor av	747	−169164.1169	−169157.8148	−7.9786	1.7036
DFT structure	1	−169170.8100	−169165.3000	−6.9715	1.4884

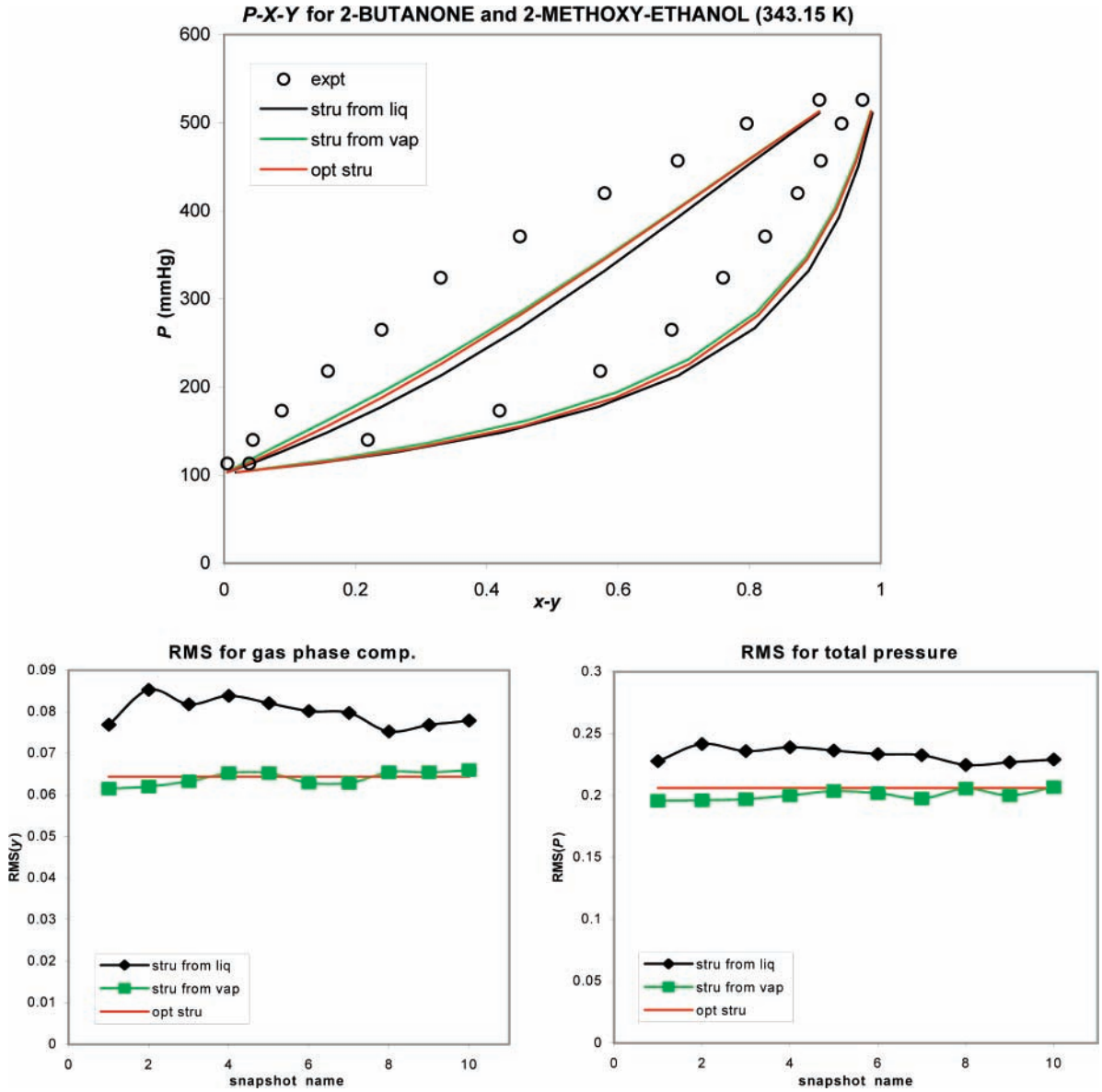

Figure 6. Pressure-composition projection and root-mean-square errors in the gas-phase composition (bottom left) and total pressure (bottom right) for the binary mixture of 2-butanone and 2-methoxy-ethanol at $T = 343.15$ K. The experimental data are taken from ref 23.

2-methoxy-ethanol the average of the logarithms of the predicted vapor pressures obtained using either the vapor and liquid structures, or the liquid and DFT structures, is significantly closer to the experimental value than the predicted vapor pressures using only one of these structures.

Since the sigma profiles and free energies change little with the environment for 1-hexanol, it is expected that very similar vapor pressure predictions will result. As shown in Table 1, the difference in the contributions to the vapor pressure from the dispersion and cavity formation energies based on the liquid and vapor structures is very small (on average, less than 0.01 log unit). Although the absolute values of these contributions obtained from the optimized structure are slightly higher, the difference in value for the three cases (structure from averaged liquid simulation, from vapor simulation, and from optimization) is small for these two terms. The restoring energy, which is calculated only from the sigma profiles, also shows only small differences among these three cases, as is also true for the ideal solvation term, which is calculated only from the energy difference between ideal gas and ideal conductor phases.

The situation is somewhat different for 2-methoxy-ethanol, since the "averaged structures" change in going from a vapor to a liquid. For the dispersion and cavity terms, the differences between using the averaged liquid ensemble, the vapor ensemble, and the optimized structure are small. However, the differences are noticeable for the ideal solvation term ($\Delta G_{i/i}^{*cco}/RT$). Splitting the $\Delta G_{i/i}^{*cco}/RT$ term into $\Delta G_{i/i}^{*is}/RT$ (energy difference between conductor and gas phase) and $\Delta G_{i/i}^{*cc}/RT$ (energy shift from original charge distribution to averaged charge distribution) as in Table 3, we see that the $\Delta G_{i/i}^{*is}/RT$ term ($\Delta G_{i/i}^{*is} = E_{COSMO} - E_{GAS}$) shows a greater variation among the three cases than the $\Delta G_{i/i}^{*cc}/RT$ term. The optimized structure results in the lowest energies in both the conductor and gas phases, followed by the structure from the average vapor ensemble, and then the structure from the average liquid ensemble. Also, the energy differences between these three structures are smaller in the conductor phase than in gas phase. There are also differences in the restoring energy term among the three structures, although these are much smaller than the difference in the $\Delta G_{i/i}^{*cco}/RT$ term (0.15 log unit difference versus 1.2 log unit difference). Therefore, for 2-methoxy-ethanol the vapor pressure predictions are noticeably different using the liquid ensembles, vapor ensembles, and

optimized structures. The main difference is due to the energy changes as a result of the environment change from the gas phase to the perfect conductor, and mostly as a result of the differences in gas-phase energies computed from each of the structures.

Structure Effect on Binary VLE Predictions. Unlike the vapor pressure predictions, which are influenced by the energy change in transferring a molecule from the gas phase to a perfect conductor, binary VLE predictions depend mainly on the difference between the sigma profiles in the mixture and of the pure compounds that are used to calculate the segment activity coefficients. We first tested predictions for the 1-hexanol and cyclohexane mixture at 354.15 K using the sigma profile for cyclohexane obtained from the DFT optimized structure in a vacuum and the reported pure component vapor pressures. As shown in Figure 5, the predicted phase diagrams for this system are almost the same using the sigma profiles obtained from the different 1-hexanol structures, as expected since sigma profiles for the different 1-hexanol structures are nearly identical. For each ensemble, the RMS values of the gas-phase composition and total pressure remain close at around 0.9% for the gas-phase composition and about 6.5% for total pressure.

The second mixture we examined is butanone and 2-methoxy-ethanol at 343.15 K. As shown in Figure 6, the phase diagrams do show differences using the structures obtained from the vapor and liquid simulations, and from DFT. The predictions using the optimized structure are close to those from the averaged vapor phase ensemble structure, and somewhat different from those using the sigma profile calculated from the liquid-phase ensemble. The differences are more apparent in the RMS deviations from experiment. The RMS errors in gas-phase composition and total pressure are higher using the averaged liquid structures than using either the averaged vapor structure or the optimized structure.

4. Conclusions

In this study, the conformation effects on the sigma profiles, the vapor pressure predictions, and the VLE predictions were investigated for two chemicals, 1-hexanol, and 2-methoxy-ethanol. For 1-hexanol, the sigma profiles vary only slightly using molecular conformations obtained from simulation of the vapor phase, from simulation of the liquid phase, and from the DFT optimized structure. However, the different conformations obtained in the same way do affect the sigma profiles for 2-methoxy-ethanol, though all have a similar general shape. Therefore, it is a reasonable first approximation to use a single molecule optimized structure for COSMO calculation instead of using structures obtained from simulation. For 1-hexanol the vapor pressure predictions using the structures obtained from liquid simulation are similar to those using the structures obtained from vapor simulation and from DFT optimization. However, for 2-methoxy-ethanol, larger differences in the vapor pressures are found when using the liquid, vapor, and optimized structures. The main difference arises from the ideal solvation energy term, and more specifically, the energy difference of the molecule in the conductor and vapor phases.

In binary mixture VLE calculations involving 1-hexanol, there is little difference in the phase equilibrium predictions when using the different structures. For the 2-methoxy-ethanol mixture, the differences in the sigma profiles lead to a more noticeable, though not a dramatic, difference in the phase equilibrium predictions. However, none of the structures led to good agreement with experiment in this case.

Overall, for simple molecules, such as 1-hexanol, there is relatively little change in the sigma profiles and properties predictions whether the molecular conformation is obtained from a single molecule DFT calculation or from a vapor or liquid simulation using a molecular mechanics force field. However, for a more complicated multifunctional molecule such as 2-methoxy-ethanol, the differences are more significant. We expect even larger differences for bigger molecules.

Acknowledgment. Financial support through Contract DE-FG02-85ER13436 of Basic Energy Sciences of the U.S. Department of Energy and Grants CTS-0083709 (S.I.S.) and CTS-0138393 (J.I.S.) from the U.S. National Science Foundation is gratefully acknowledged. Parts of the simulations were carried out using resources provided by the Minnesota Supercomputing Institute.

References and Notes

(1) Gmehling, J. *Fluid Phase Equilib.* **1998**, *144*, 37.
(2) Katritzky, A. R.; Lobanov, V. S.; Karelson, M. *Chem. Soc. Rev.* **1995**, *24*, 279.
(3) Allen, M. P.; Tildesley, D. J. *Computer Simulation of Liquids*; Oxford University Press: Oxford, 2001.
(4) Tomasi, J.; Persico, M. *Chem. Rev.* **1994**, *94*, 2027.
(5) Cramer, C. J.; Truhlar, D. G. *Chem. Rev.* **1999**, *99*, 2161.
(6) Klamt, A. *J. Phys. Chem.* **1995**, *99*, 2224.
(7) Klamt, A.; Jonas, V.; Burger, T.; Lohrenz, J. C. W. *J. Phys. Chem. A* **1998**, *102*, 5074.
(8) Lin, S. T.; Chang, J.; Wang, S.; Goddard, W. A. I.; Sandler, S. I. *J. Phys. Chem. A* **2004**, *108*, 7429.
(9) Lin, S. T.; Sandler, S. I. *Ind. Eng. Chem. Res.* **2002**, *41*, 899.
(10) Klamt, A.; Eckert, F. *Environ. Toxicol. Chem.* **2002**, *21*, 2562.
(11) Klamt, A.; Eckert, F.; Diedenhofen, M.; Beck, M. E. *J. Phys. Chem. A* **2003**, *107*, 9380.
(12) Putnam, R.; Taylor, R.; Klamt, A.; Eckert, F.; Schiller, M. *Ind. Eng. Chem. Res.* **2003**, *42*, 3635.
(13) Klamt, A.; Eckert, F.; Hornig, M.; Beck, M. E.; Burger, T. *J. Comput. Chem.* **2002**, *23*, 275.
(14) Siepmann, J. I.; Frenkel, D. *Mol. Phys.* **1992**, *75*, 59.
(15) Martin, M. G.; Siepmann, J. I. *J. Phys. Chem. B* **1999**, *103*, 4508.
(16) Panagiotopoulos, A. Z. *Mol. Phys.* **1987**, *61*, 813.
(17) Martin, M. G.; Siepmann, J. I. *J. Phys. Chem. B* **1998**, *102*, 2569.
(18) Chen, B.; Potoff, J. J.; Siepmann, J. I. *J. Phys. Chem. B* **2001**, *105*, 3093.
(19) Stubbs, J. M.; Potoff, J. J.; Siepmann, J. I. *J. Phys. Chem. B* **2004**, *108*, 17596.
(20) Klamt, A.; Jonas, V. *J. Chem. Phys.* **1996**, *105*, 9972.
(21) Boublik, T.; Vega, C.; Diazpena, M. *J. Chem. Phys.* **1990**, *93*, 730.
(22) Walsh, J. M.; Gubbins, K. E. *J. Phys. Chem.* **1990**, *94*, 5115.
(23) Gmehling, J. In *Vapor-liquid equilibrium data collection*; DECHEMA: Frankfurt/Main, 1977 and onward.